International Journal of Scientific Research and Engineering Development – Volume 2 Issue 4, July – Aug 2019

Available at www.ijsred.com

RESEARCH ARTICLE OPEN ACCESS

Effects of SiO_x Aging Time on Nano Crystalline Silicon Thin Film for Optoelectronic Devices using Sol-Gel Method

Moniruzzaman Syed*, Brittany Anderson*, Joe Mvula*, Yahia Hamada*, Muhtadyuzzaman Syed** and Tej Prasad Poudel***

*Division of Natural and Mathematical Sciences, Lemoyne Owen College, Memphis, TN, USA
Email: Moniruzzaman_syed@loc.edu
**Department of Electrical and Computer Engineering, Purdue University, West Lafayette,IN, USA
Email: Msr512@gmail.com
***Department of Physics and Material Science, University of Memphis, Memphis, TN, USA
Email: tppoudel@uom.edu

Abstract:

Nano silicon powders were prepared by the grinding technique and subsequently mixed in sol-gel of Tetraethylorthosilicate (TEOS) and ethanol solution. The silicon dioxide films synthesized from the sol-gel solution were preliminary studied in the term of the optical property such as refractive index (n) by varying the aging time and annealing temperatures. By using a Fourier transform infrared spectroscopy technique, the obtained x-composition values of the SiOx films were extended from 1.1 to 2.0 with an increasing time of the aged sol-gels. In addition, the lower x-composition value can be controlled by increasing the annealing temperatures from 100°C to 450°C. The prepared films from the precursor of nano-silicon powder suspension were characterized by Raman spectroscopy, XRD, AFM and SEM measurements in order to obtain more understanding of the chemical composition and silicon nano-crystallite quality, respectively. The average size of Si powder and nc-Si dots in SiO_2 was estimated in the order of ~10 nm and ~8.33 nm, respectively. Average uniform grain size was estimated by ~5.4 nm. Minimum career mobility and maximum resistivity were observed as ~37.5 cm^2/v.s and ~7.35 Ω-cm respectively at higher aging time.Crack-free surfaces of nc-Si thin film have been observed successfully in SiO_2 phase. Spectral broadening and the frequency downshifting from 525.35 cm^{-1}werespeculated to be caused by the quantum size effect.

Key Words: **Silicon, Thin Film, Sol-gel and Silicon Oxide**

I. INTRODUCTION

Nanocrystalline silicon (nc-Si) thin films are thought to be promising structures with a wide range of applications in many fields. One such field is of optoelectronic devices like solar cells, light emitting diodes (LEDs), lasers, sensor devices and thin film transistors[1-3]. Silicon (Si) as an optically active layer was appeared to be impossible to utilize properly because of its indirect band gap. However, in recent years, nc-Si materials are showing many revolutions of photonic functions[4] and the quantum confinement effect (QCE) of charge excitons in the silicon nanostructure is leading to a quasi-direct transition [5]. One of the main reasons to form Si low-dimensional structure is its compatibility with the manufacture know-how of integrated circuits (ICs). Moreover, QCE in Si-nanostructures founds to be another approach in

 ©IJSRED: All Rights are Reserved

engineering a quasi-direct transition having the visible light emission at room temperature. In particular, the nc-Si band gap energy (Eg) can be elongated in order to shifting down the valence states and to shifting up of the conduction states once the small nanometric size approaches the size of its Bohr exciton radius. The band gap modification due to the quantum confinement will be given in a simple effective mass approximation as follows:

$$\Delta Eg \propto \frac{1}{m.a^2} \quad (1)$$

where m is an effective isotropic mass in the confinement direction, and a is a nanoparticle size.

Shockley-Read-Hall recombination mechanism of nc-Si material at room temperature for optoelectronic devises as promising caused by the size confinement is playing very important role and which is suppressed because of carriers become localized and are not able to diffuse to defects[6)]. Auger recombination is not present until two excitons are generated within the same nanocrystals. Furthermore, radiative recombination becomes more efficient since the electron-hole wavefunctions overlap overwhelmingly in space causing faster recombination. These recombination behaviors have led to been widely investigated in the structural, electronic, and optical properties of nanocrystal materials.Especially, the systems composed of nc-Si embedded into its dielectric materials such as its oxides, nitrides, and carbides. They present a promising alternative to tunable band gap from 1.2- 2.0 eV [7)].

Various conventional deposition techniques such as plasma enhanced chemical vapor deposition (PECVD)[8)], RF magnetron sputtering[9)], Ion implantation[10)] and so on have been used to deposit nc-Si:H thin films which are compatible with the standard Si technology. However it is very difficult in achieving concentrations high enough to obtain efficient optical properties. Many techniques mentioned above have been found to be expensive and time consuming because of the production under high vacuum and/or annealing processes. A sol-gel method is quite inexpensive and easy to fabricate such Si nanocrystals embedded into its dielectric matrix. The sol-gel method by centrifugal processing has been recommended as a technique to be achieved in this objective [11)]. The sol-gel was used as a viscous medium through Si crystallites settle. Nevertheless, the centrifugal processing might produce a bulk material which has such a functional limitation for thin film optoelectronic devices.

In this research article, using sol-gel spin coating procedure, we prepared nc-Si thin films in the formation of nanocomposite materials. The prepared silicon nanostructure consists of the nano-Si powders, which were isolated in a continuous silicon dioxide phase. P -type (100) Si wafer as nano-Si powders precursor was appropriately grinded for our work. The prepared SiO_2 buffer layer by synthesizing the sol-gel is a crucial stack of the layers for our work. Furthermore, the investigation step of boron doped in the nc-Si dots/SiO_2 film is a very important towards a realization of a nano-scaled p n junction device. For a compositional analysis, the chemical bonding environment of boron was investigated by the FT/IR. The crystal structure of nanometer Si dots embedded into the silicon oxide was studied by the measurement of Raman spectra, XRD, Ellipsometry, Four-point probe and Uvis.

II. EXPERIMENTAL

A. Substrates preparation

Nano-crystalline silicon thin films were prepared by the sol–gel spin coating technique. Fig. 1a shows the block diagrams of step by step experimental procedure at a glance. Fig. 1b shows the spin-coater set up used in this experiment. Nitrogen (N_2) gas cylinder as a back pressure is connected to the liquid dispenser. Sol-gel liquid holder is also connected to the liquid dispenser with a stand just above the spin coater stage as shown in Fig 1b. Adjusting the back

 ©IJSRED: All Rights are Reserved

pressure, the amount of precursor liquid (0.2 ml) can be disseminated on the mounted substrate in the spin coater. In these work, different substrates (Corning 7059 and Si wafer) were used for different measurements. The sample preparation processes can be divided into two steps: (1) The substrates were cleaned for 15 min using acetone, 15 min using ethanol and 15 min using DI water in an ultrasonic cleaner, (2) preparing the sol-gel oxide buffer layer and nc-Si sol-gel solvent-solutions as well and (3) finally, nc-Si thin films were prepared by changing various aging time (1 day, 5 days, 7 days and 8 days) at room temperature (RT). The conditions of substrates cleaning and film deposition are summarized in Table I & II.

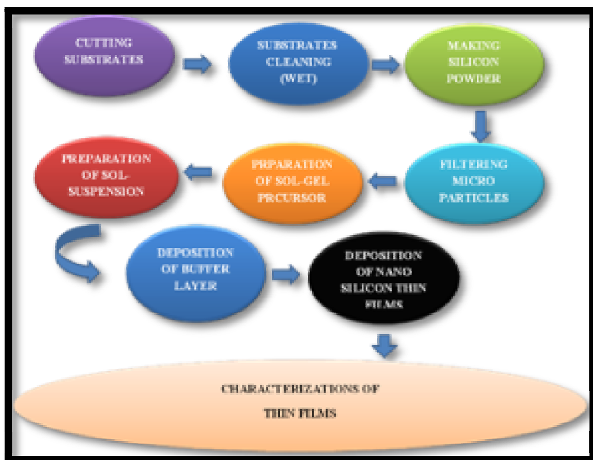

(a)

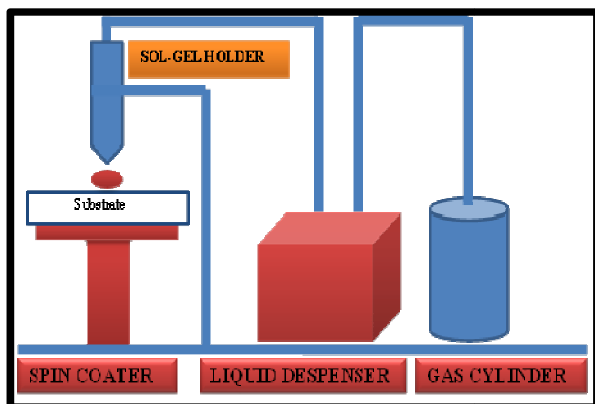

(b)

Fig.1 (a) Overall steps and (b) Schematic diagram of the Spin coater set up used in this experiment

B. Preparation of Nano-Si powders

The nano-Si powders were produced from (100) p-type mono-crystalline Si wafer under long time (4-7 hrs) grinding process having the boron impurity in the order of 1-20 Ω-cm. Si-powders then mixed with ethanol absolute and filtering through a sieve with pore radius 40 µm.

C. Creation of nano-crystalline Si thin films using sol-gel method

Fig. 2 shows the schematic representation of the sol-gel method. This process can be divided in to different steps.

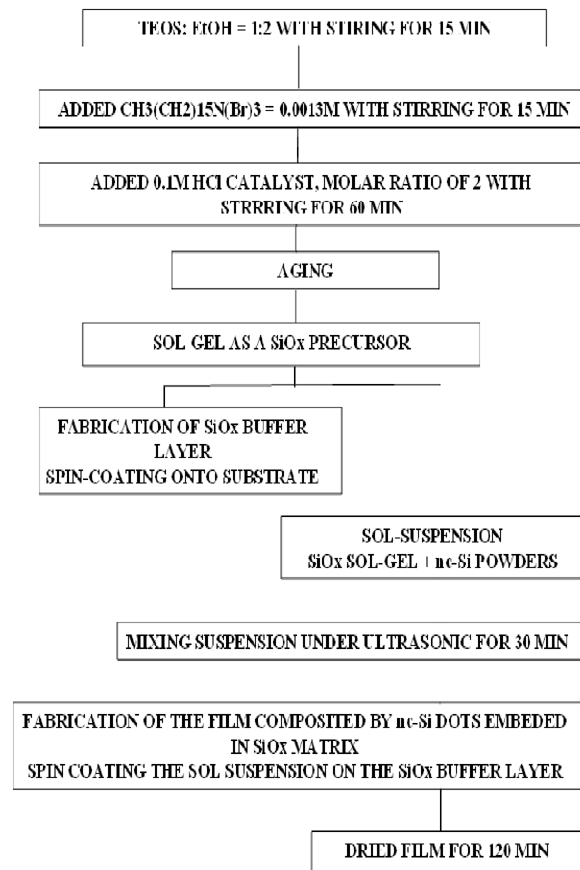

Fig. 2 Schematic representation of the sol-gel method

1) Preparation of silicon oxide buffer layer

Silicon oxide precursor: Tetraethylorthosilicate, $Si(OC_2H5)_4$ (TEOS, 98% Fluka) and ethanol

 ©IJSRED: All Rights are Reserved

absolute, (C_2H_5OH, 99% BDH) (EtOH)) were used as a **silicon oxide precursor**.

Buffer Layer: In fabrication of Si oxide buffer layer, the dielectric sol-gel was first prepared as follows: 1 mole of TEOS (8.33 mL) and 2 moles ofEtOH (3.69mL) were mixed and then stirred for 15 min at the room temperature.

Surfactant: CetylTrimethyl Ammonium Bromide, $C_{19}H_{42}BrN$ (CTAB, 99% Sigma Aldrich) was used as **surfactant**. In addition, 0.0013M CTAB and 0.1M HCl catalysts in water were subsequently added dropwise to the solution until the water to TEOS molar ratio of 2. The condensation of TEOS at about pH 2 was controlled by adding HCl catalyst. The proper solutions were then stirred at room temperature for 60 minutes.

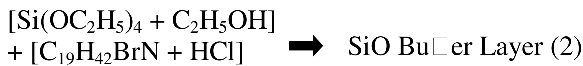

$[Si(OC_2H_5)_4 + C_2H_5OH] + [C_{19}H_{42}BrN + HCl] \rightarrow$ SiO Bu□er Layer (2)

2) Preparation of Sol-gel Suspension

In order to obtain the suspension uniformity, sol-suspension was prepared from mixture of nano-scaled Si powders (0.05 g) with TEOS solution (5ml) under an ultrasonic for 30 min. The preparing process of sol-suspension is shown in Fig. 3.

3) Synthesis of Thin films

After aging of the gel for 1 day, 0.2 ml of the prepared TEOS gel as a Si-oxide precursor was spun at 11,800 rpm for 10 s on both substratesin accordance with the process shown in Fig. 1b. The acquired Si-oxide is an important buffer layer in order to have a good coherence between its surface and the sol-suspension for the next step. To inhibit the crack of the bu□er layer structure, the first Si-oxide film was suitably dried for 2 hours on a hot plate in air ambient at 100°C. Afterward, 0.2ml of sol-suspension was released from the sol-gel holder located just above the spin coater on the dried oxide buffer layer and nc-Si thin film deposition was performed by spinning the coater for 10 s with same rpm of 11,800 as above. Under properly sequence process, B-doped Si nanocrystallites embedded in a continuous oxide dielectric phase were expected to obtain in this work (Fig.3).

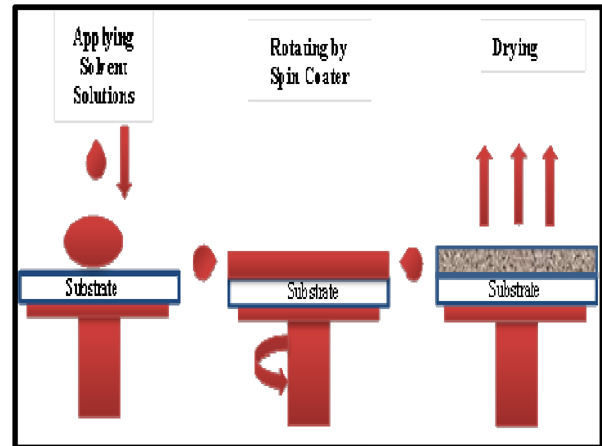

(a)

(b)

Fig. 3 (a) Stages of thin film deposition by spin coating method and (b) schematic of the Cross-section of prepared thin film.

Table I: Wet cleaning Conditions used to disinfect substrates and remove any fragments of material of oil.

Substrates	Acetone	Ethanol	DI-Water
P-type (100)	15 min	15 min	15min

 ©IJSRED: All Rights are Reserved

Silicon			
Corning 7059 Glass	15 min	15 min	15min

Table II: Deposition Conditionsof nc-Si thin film growth using Sol-Gel method

Substances	Quantity
TEOS (1 mole)	8.33 mL
EtOH (2 mole)	3.69 mL
0.0014 M CTAB	0.2 gm
Di-Water	200 mL
CTAB +TEOS Sol.	6.01 mL
0.1M HCl + TEOS Sol.	6.01 mL
nc-Si powder	0.05 gm
Add SiOx Sol-Gel	5.0 mL
Spin-Coater rpm	11,800
Deposition Time (SiOx& Thin Film)	10 sec
Aging Time of SiOx Sol-Gel	**VARY**

4) Stoichiometry of SiOx buffer layer

The stoichiometry of as-deposited SiOx was estimated from shifts of the asymmetric Si-O-Si stretching peak with adjacent O-atoms in the IR absorption spectra. The change in chemical bonding state of Si oxide film was also analyzed by using Fourier transform infrared spectroscopy, FT-IR (Perkin-Elmer System 2000)with a wavenumber resolution of 2 cm^{-1} as the following equation:

$$\eta = 978.72 + 30.63x \quad (3)$$

where η is a position of peak frequency (cm^{-1}) and x is stoichiometry of SiO_x film.

D) Characterizations of the thin films

The structural properties were investigated using an XRD instrument (SIEMENS D5000 X-ray diffractometer, λ = 1.54 Å). The XRD spectra were recorded in the 2θ range from 20° to 80° at a fixed grazing angel of 5° and a scan rate of 0.02°/s. In the present study, any difference in the film thickness was corrected using the X-ray absorption coefficient for Si. Thus, the XRD intensities observed for different films can be compared. The average crystallite size, [δ], was estimated from the width of the XRD spectra using Scherrer's formula as follows:

$$[\delta] = \frac{k\lambda}{\beta\cos\theta} \quad (4)$$

where k, λ, β and θ are a constant, the wavelength of X-ray (1.54 Å), the full width at half maximum (FWHM) and Bragg angle of the diffraction peak respectively.

The Raman spectra of the films were recorded using a portable iRaman (B&W TeK) with the argon ion laser having an excitation wavelength of 514 nm was used and the power was less than 5 mW. Crystalline volume fraction [ρ] has been estimated from the deconvolution of the spectra at around 480cm^{-1} and 580 cm^{-1} respectively using the following equation:

$$[\rho] = \frac{I_{580}}{\alpha(I_{580}+I_{480})} \quad (5)$$

where I_{580} and I_{480} are integrated intensities of the Raman peaks corresponding to crystalline and amorphous phases respectively. The factor α is generally equal to 1 for nc-Si films. The crystallite size of the Si nanocrystallites in the films can be estimated using the following equation:

$$[\Omega] = 2\pi\sqrt{\frac{B}{\Delta\omega}} \quad (6)$$

where B is 2.24$cm^{-1}nm^2$ for Si and Δω is the peak shift compared to c-Si peak located ~580 cm^{-1}.

The surface morphologies of nc-Si:H films were examined by AFM (Agilent 5500 non-contact mode). The topological images were taken by scanning electron microscopy (SEM, 1450VP, Phenom Pure).

 ©IJSRED: All Rights are Reserved

The IR absorption was measured by a Thermo Scientific, Nicolet iS10 FTIR spectroscopy with the wavenumber range of 400 to 4,000 cm^{-1} and resolution of 2 cm^{-1}. Thickness of the films was obtained by using an ellipsometer (Rudolph Research, Ellipsometer Auto EL-III) with a wavelength of 632.8 nm.

III. RESULTS

1) Structural Analysis by Raman Scattering

In order to understand the quality (i.e. crystallinity) of silicon powders and nc-Si thin films, Raman spectroscopy technique was used in this experiment. Fig. 4a shows the Raman spectra of as-synthesized silicon (p-type, <100>, B-doped, 1-20 Ω-cm) powders. Sharp peak centered at 518.23 cm^{-1} is clearly indicating the crystalline phase.

(a)

(b)

Fig. 4 (a) Si powder shows a wave number of 518. 23 cm^{-1} confirming a crystalline structure and (b) Raman Spectra for Si films show the significant peaks in the nc-Si phase for days 7 and 8.

Fig. 4b shows the Raman spectra of nc-Si thin films as a function of aging time [£] = 1day, 5days, 7days and 8 days.It is found that the Raman spectra of nc-Si films for day 1 and 5become asymmetric broadening and peaks shift downward from 529.9 cm^{-1}causing by stress and strain in the film, suggesting the formation of microcrystalline silicon phase[12)]. However, size confinement results in uncertainty of the phonon momentum, thus leading to a downshift and asymmetric broadening of the Raman spectra[13)]. For the thin films on day 7 and 8, sharp peaks at ~530 cm^{-1} are observed clearly indicating the presence of nc-Si.

Fig. 5 shows the crystallites size and Full Width Half Maximum (FWHM) as a function of [£]. For the size approximation, we used the analytic equation as follows[14)]

$\Delta\omega = -A\left(\frac{\alpha}{L}\right)^{\gamma}$ (7)where A = 47.41 cm^{-1},γ = 1.44, $\alpha$is the silicon lattice parameter (α = 0.543 nm), L is silicon dot diameter, and Δω is the shift frequency.

 ©IJSRED: All Rights are Reserved

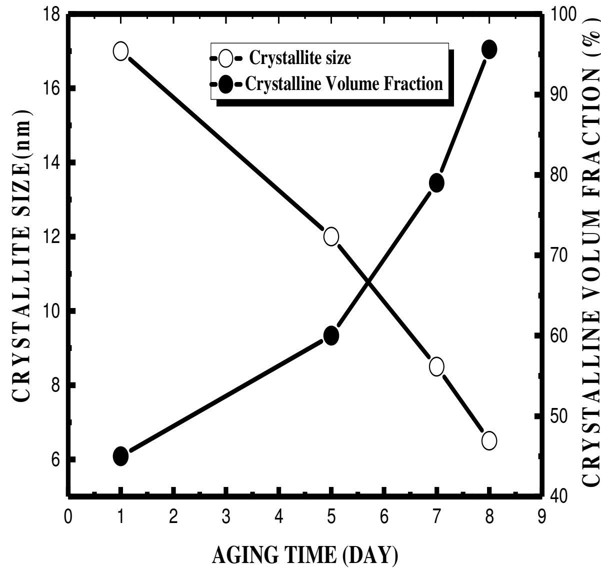

Fig. 5 shows the crystallite size and crystalline volume fraction as a function of [£].

As shown in this fig. 5, crystallites size is getting decreased with increasing aging time having the lowest (6.5 nm) at 8days. On the other hand, crystalline volume fraction [ρ] has been found to be increased with the increment of [£] having the maximum value at 8th day ([ρ] = 95%).

2) Structural Analysis by X-ray diffraction (XRD)

Fig.6 shows theXRD spectra of nc-Si thin films as a function of [£]. (111), (220) and (311) planes are observed for all the samples except 1 and 5 days (Fig. 6). An increased in the relative intensity of the (220) XRD spectra is found to correspond well with an increased in the intensity of 530 cm^{-1} component (crystalline phase) in Raman spectra under 7 and 8 days. (110) crystallite size was found to be ~ 5.3 nm at 8th day, which corresponds well with an increased (110) XRD relative intensity, decreased XRD width (FWHM) and which has the largest crystallinity.

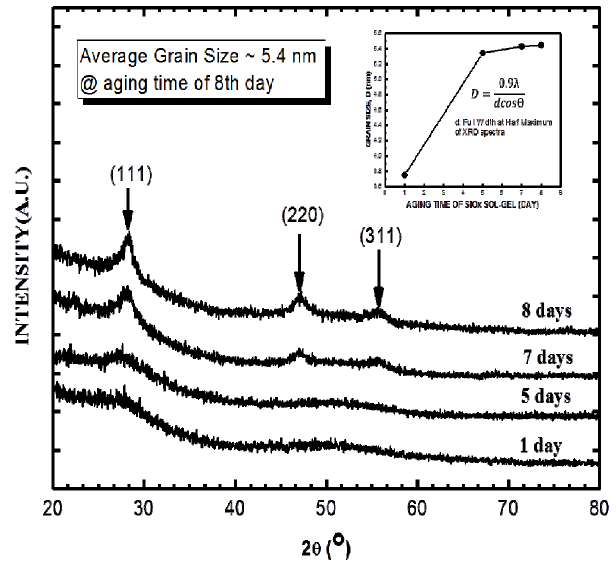

Fig. 6 XRD spectra of nc-Si films shows significant peaks in (111), (220), and (311) for days 7 and 8 with a grain size of 5.4 nm at the aging time of 8 days.

3)Bonding analysis byFT/IR Spectra

The IR absorption spectra over the range of 400-4000 cm^{-1} for films deposited with different [£].The spectra at around 453.47 cm^{-1}, 747.97 cm^{-1}, 902.49 $cm^{-1}$and 1541.66 cm^{-1} are assigned to Si-O Rocking, Si-O bending,Si-O stretching and adjacent O-atom out of phase absorption bands, respectively.

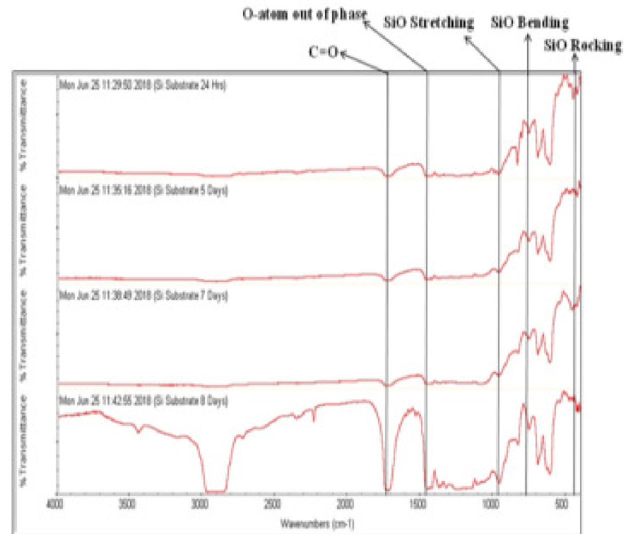

(a)

©IJSRED: All Rights are Reserved

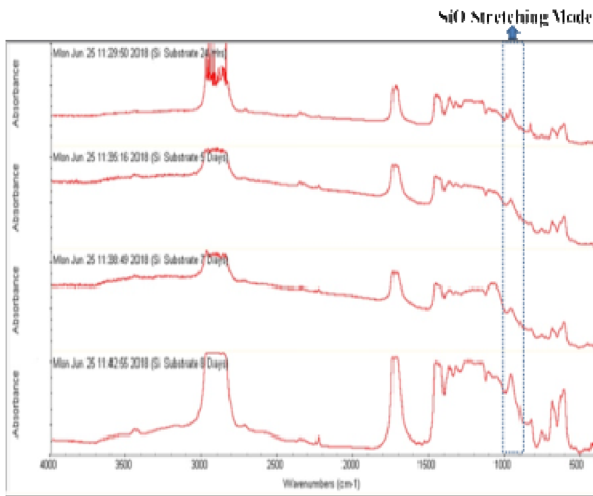

(b)

Fig. 6FT/IR (a) transmittance spectra and (b) absorption spectra of nc-Si thin film as a function of aging time.

Figure 7 shows the peak position of absorbance and x-composition of SiO_x as a function of aging time.The x-composition of SiO_X for different aging time was calculated using the formula explained before. It has been found that the x-stoichiometry of SiO_x is expected to be in the range of ~1.1 to ~2.0. Therefore, we apply the SiO_2 as a medium dielectric phase of nc-Si film.

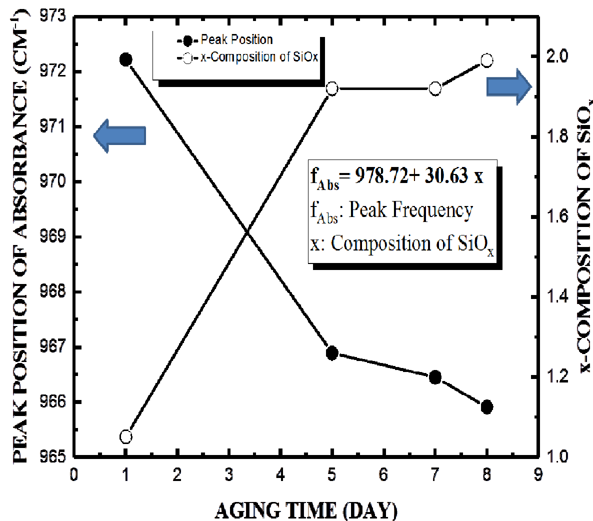

Fig. 7An analysis of peak position and x-composition of the SiO_xfilms with different aging time.

4)Structural Analysis by AFM

Fig. 8 shows the AFM micrographs of nc-Si thin films deposited at day-8 as a function of aging time under (a) 1-day, (b) 5-day, (c) 7-day and (c) 8-day.

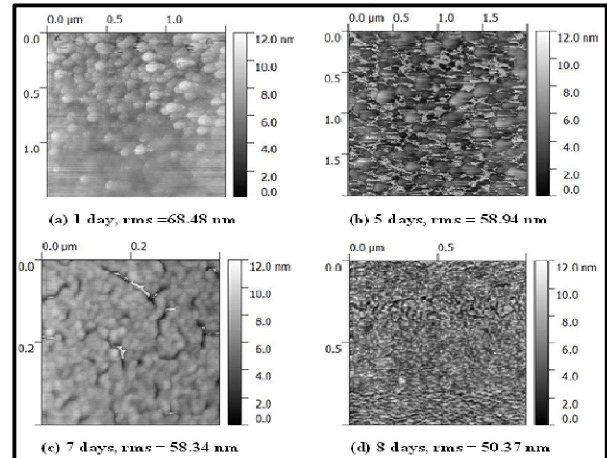

Fig. 8AFM micro graphs of nc-Si thin film show increasing homogeneity as the samples approach 8 days aging.

The degree of surface roughness is the root mean square (rms) value of the roughness heights. It is reveals that the roughness of the nc-Si films are found to be 68.48 nm for 1-day, 58.94 nm for 5-day, 58.34 nm for 7-day and 50.37 nm for 8-day respectively. As shown in these diagrams at 8-day, surface roughness is largely reduced and the roundish-like roughness having uniform heights with homogeneous grains distribution were observed. These results are well consistent with the results of Raman and XRDmeasurements.

5)Structural Analysis by Scanning Electron Microscope

Fig. 9 shows the SEM micro graphs of nc-Si thin films as a function of aging time. It is a branch of microscopy that produces images of a sample by scanning the surface with a focused beam of electrons. The electrons interact with atoms in the sample, producing various signals that contain information about both the sample's surface morphology and composition. As shown in Fig.

 ©IJSRED: All Rights are Reserved

9a, ununiformed larger island-type of micro-structured was observed for the film deposited in 1day.

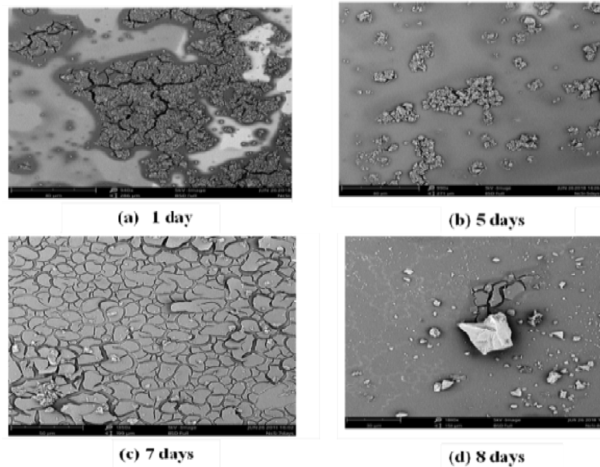

Fig.9 SEM of nc-Si:Hthin films show a shift from micro to nanoparticles by day 8 aging.

In day 5, it has been transformed to smaller nano-structured islands with homogeneous surface. However, day 7, uniform nano-structured grains were observed having larger grain-boundaries. In day 8, crack free uniform grains were observed which was showing the highest crystallinity.

6) Annealing effects on the thickness and refractive Index

Refractive index of the prepared dielectric film is very important parameter in order to provide its optical information. Fig. 10 shows the influence of annealing temperatureof the film deposited at day 8 on the thickness and refractive index values of the film. By increasing the annealing temperature, the average value of the refractive index exhibits a slight increase from 1.30 – 1.60.

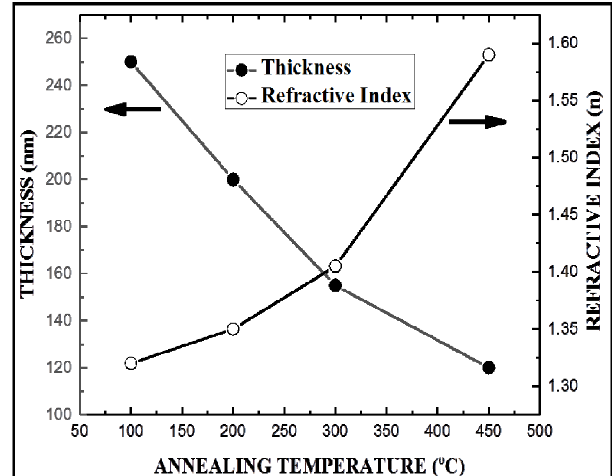

Fig.10shows the change of thickness and refractive index as a function of annealing temperature.

It might be contributed to start of pore removal and densification which is similar to Fardad's work [15]**.** Moreover, the film thickness gradually shrinks from 260nm to 120 nm.It is mainly due to the shrinkage of the gels during drying and it is forced by capillary pressure of the small pore liquid[16]. Using annealing temperature, the surface tension between liquid and vapor is playing very important role. Therefore, the less shrinkage of as-deposited film and also the film annealed at 100°C can lead to the less crack or crack free.

7) Influence of aging time on the thickness and refractive Index of SiO_xfilm

Fig. 11 shows the influence of aging time on the average thickness and refractive index of SiO_xfilm at low drying temperature (100°C) showing the same crack free tendency.

 ©IJSRED: All Rights are Reserved

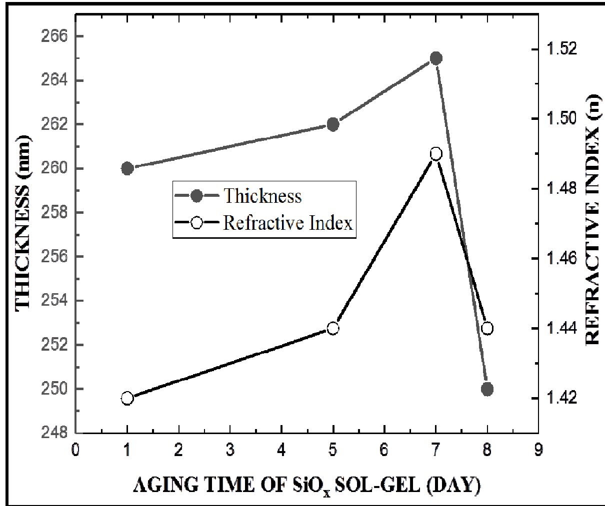

Fig. 11shows the change of thickness and refractive index of SiO_x film as a function of aging time.

With longer aging time, the thickness increases as a consequence of a more gel viscosity. For 8-day aging time, thickness and refractive index reversible drop possibly due to that EtOH as a solvent evaporates, causing shrinkage of the gel network. The refractive index of the prepared film by the sol-gel method shows in the range of 1.38-1.49.

8) Evaluation of electrical properties of nc-Si thin film based on Resistivity and Hall mobility measurements

Fig. 12 shows the variation of hall mobility and the resistivity of nc-Si thin films as a function of aging time. The resistivity ∅ of the films was calculated from four-point probe:

$$R = \emptyset \frac{L1}{dL2} \quad (8)$$

where L_1 is the length, L_2 is the width, d is the thickness and R is the resistance between the cross sections (left side and the right side of the sample). Mobility and resistivity are showing opposite relationships to each other having the minimum mobility of ~37.5 cm^2/v.s and themaximum resistivity of ~7.35 Ω-cm at higher aging time, respectively.

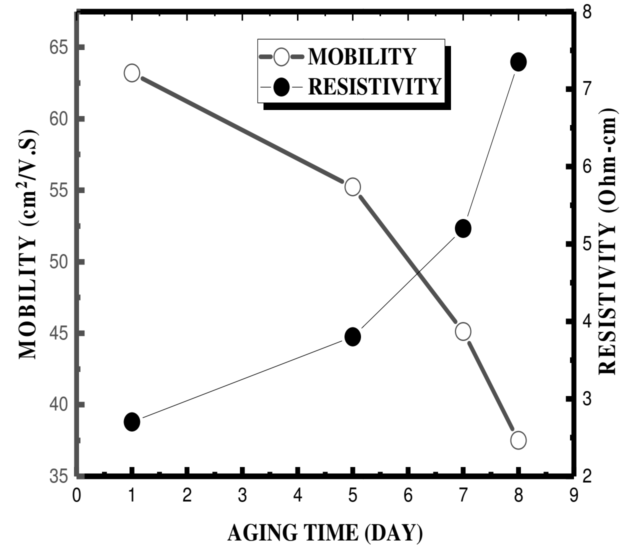

Figure 12 Mobility and Resistivity measurements of nc-Si:H films deposited on glass substrates at aging time.

VI) CONCLUSION

Sol-gel nano-crystalline silicon thin film embedded in SiO_2 matrix was prepared using spin-coating technique as a function of aging time. Optimal crystallinity was observed at the aging time of day-8 according to the FT/IR and refractive index measurements. Crack-free surfaces of nc-Si thin film have been observed successfully in SiO_2 phase. The average size of synthesized Si powder and nc-Si dots in SiO_2 was estimated in the order of ~10 nm and ~8.33 nm, respectively. Average XRD grain size was estimated by ~5.4 nm.Minimum mobility of ~37.5 cm^2/v.s and the maximum resistivity of ~7.35 Ω-cm were observed at higher aging time. The obtained nc-Si films show the good quality of the Si crystal by Raman measurements. We achieved to prepare the thin film with crack-free nc-Si dots in SiO_2 phase at higher aging time.

ACKNOWLEDGMENT

The authors would like to thank Dr. Sherry Painter, division chair of LeMoyne-Owen College for her support during this work. Special thanks to Dr. Delphia Harris, professor of chemistry at LeMoyne-Owen College for her helpful suggestions. The authors would also like to thank Dr. Sanjay Mishra, Department of Physics and Material Science, University of Memphis for using characterization tools. We would also like to acknowledge the financial support from NSF (Grant # HRD- 1332459).

REFERENCES

[1] J.-H. Shim, ImSeongil, Kim YounJoong, N.-H. Cho, (2006) "Nanostructural and optical features of hydrogenated nanocrystalline silicon films prepared by aluminium-induced crystallization" Thin Solid Films, 503, 55

[2] H. Shirai, T. Arai, T. Nakamura, (1997) "Control of the initial stage of nanocrystallite silicon growth monitored by in-situ spectroscopic ellipsometry"Appl. Surf. Sci. 113(114), 111

[3]J.P. Kleider, C. Longeaud, R. Bruggemann, F. Houze, "Electronic and topographic properties of amorphous andmicrocrystalline silicon thin films" (2001) Thin Solid Films 383, 57

[4] Z.H. Lu, D.J. Lockwood, and J.M. Baribeau (1995) "Quantum confinement and light emission in SiO_2/Si superlattices" Nature, 378, pp. 359.

[5] M. Pe´ralvarez, J. Barreto, J. Carreras, A.Morales,D.N. Urrios, Y. Lebour, C.Dom`ınguez, and B Garrido (2009) "Si-nanocrystal-based LEDs fabricated by ion implantation and plasma-enhanced chemical vapor deposition," Nanotechnology,20,405201

[6] J. Linnros (1999) "Silicon-based microphotonics from basics to applications," IOS Press, Amsterdam, pp. 47-85.

[7] G. F. Grom, D. J. Lockwood, J. P. McCaffrey, H. J. Labbe, P. M. Fauchet, B. White, Jr., J. Diener, D. Kovalev, F. Koch, and L. Tsybeskov, "Ordering and self-organization in nanocrystalline silicon" (2000) Nature, 407, pp. 358.

[8] F. Iacona, C. Bongiorno, C. Spinella, S. Boninelli, and F. Priolo, (2004) "Formation and evolution of lumi-nescent Si nano clusters produced by thermal an-nealing of SiO_x films," Journal of Applied Physics, 95, pp. 3723-3732.

[9] P.M. Fauchet, J. Ruan, H. Chen, L. Pavesi, L. Dal Negro, M. Cazzaneli, R.G. Elliman, N. Smith, M. Samoc, and B. Luther-Davies, (2005) "Optical gain in different silicon nanocrystal systems," Optical Materials, 27, pp.745-749

[10] K.S. Min, K.V. Shcheglov, C.M. Yang, H.A. Atwater, M.L. Brongersma, and A. Polman, (1996) "Defect-related versus excitonic visible light emis-sion from ion beam synthesized Si nanocrystals in SiO_2," Applied Physical Letters, 69, pp. 2033-2035.

[11] D.J. Duval, B.J. McCoy, S.H. Risbud, Z.A. Munir, (1998) "Size selected silicon particles in sol-gel glass by centrifugal processing," Journal of Applied Physics, 83, pp. 2301-2307.

[12] G. H. Loechelt, N. G. Cave, and J. Menendez, (1995) "Measuring the tensor nature of stress in silicon using polarized off-axis Raman spectroscopy," Ap-plied Physical Letters, 66, pp. 3639

[13] H. Richter, Z. P. Wang, and L. Ley, (1981) "The one phonon Raman Spectrum in microcrystalline sili-con", Solid stat commun., 39, pp. 625.

[14] J. Zi, H. Bscher. C. Falter, W. Ludwig, K. Zhang and X. Xie, (1996) "Raman shifts in Si nanocrystals," Applied Physical Letters, 69, pp.200.

[15] M. A. Fardad, "Catalysts and the structure of SiO_2 sol-gel films," Jourmal of Materials Science, 35, pp. 1835-1841, 2000.

[16] A. SoleimaniDorcheh, and M.H. Abbasi, "Silica aerogel; synthesis, properties and characterization", Journal of materials processing technology,199, pp. 10-26, 2008.